Inverse Problems, Design and Optimization Symposium
Rio de Janeiro, Brazil, 2004

BUCKLING OPTIMIZATION OF COMPOSITE PLATES SUBJECTED TO UNCERTAIN THERMAL AND NONUNIFORM MECHANICAL LOADINGS

Alfredo R. de Faria and Sérgio Frascino M. de Almeida
Department of Mechanical Engineering
Instituto Tecnológico de Aeronáutica, ITA
São José dos Campos, SP, Brazil
arfaria@mec.ita.br and frascino@mec.ita.br

ABSTRACT

Composite rectangular plates are traditionally optimized for buckling assuming that perfectly uniform loadings are applied. However, this assumption is clearly not realistic for composite structures in real applications, particularly when the multiplicity of potential load cases is considered. Composite plate optimization is addressed differently in this paper: the loading distribution is not assumed to be uniform but it is allowed to vary within an admissible set, conferring uncertainty to the applied loads. The admissible load space comprises loadings that can be represented through a collection of piecewise linear functions defined along the plate edges. The uncertainty of the loading is treated with the aid of a minimax formulation where the loading configuration and piecewise constant plate thicknesses are taken simultaneously as design variables. The choice of design variables imply in variable thickness non-homogeneous composite plates characterized by nonzero thermal residual stresses, inherited from the thermal processing. These residual stresses must also be accounted for in the buckling calculation as they significantly affect elastic behavior of the plate. The optimal composite plates obtained by the present optimization strategy satisfactorily withstand not only perfectly uniform loadings but an entire class of piecewise linear loadings.

NOMENCLATURE

$\mathbf{f}_p$	prebuckling force vector
$\mathbf{f}_t$	thermal load vector
h_{2i}, h_{2i-1}	outer ply thicknesses
$\bar{h}$	base plate thickness
$\mathbf{h}$	vector of reinforcement heights
$\mathbf{K}$	stiffness matrix
$\mathbf{K}_t$	thermal geometric stiffness matrix
$\mathbf{K}$	geometric stiffness matrix
m	number of basis functions
$\mathbf{q}$	eigenvector
$\mathbf{q}_p$	prebuckling displacement vector
$\mathbf{q}_t$	thermal displacement vector
R_i	loading component
$\mathbf{r}$	vector of uncertain loads
ΔT	temperature difference
λ	buckling load

INTRODUCTION

Composite beams, plates and shells are widely used in the aerospace industry because of their advantages over commonly used isotropic structures specially when it comes to weight savings. The large specific stiffness and resistance associated with composites allows for the manufacture of highly slender beams, and thin plates and shells. This slenderness or thinness makes aerospace composite structures prone to elastic instability. Therefore, buckling analyses of composite structural components must be performed in order to ensure, for instance, that a composite panel designed to be part of a control surface does not buckle thereby compromising its aerodynamic shape.

Optimization of composite structures has been performed in the past [1-5] using diverse sets of design variables such as number of plies, ply thickness, continuous ply orientation, discrete ply orientation, reinforcement height and position, and lamination parameters. The common aspect of these studies is the fact that all of them assume that a fixed loading configuration exists and the load magnitude, usually denoted by λ, is the objective function to be maximized subjected to a number of constraints. The example of a plate under biaxial loading illustrates the point. In this case a constant load ratio is assumed such that the

uniform normal loads along the *x* and *y* axes hold a constant relationship.

Despite the availability of digital computers it is still common practice to use tables and diagrams found in aircraft design manuals [6, 7] to calculate buckling loads of isotropic and orthotropic plates. However, one assumption is almost always present in those calculations, namely, the applied loading is uniformly distributed along the plates' edges. This assumption has historical motivations since the prebuckling stress distribution is relatively simple if the loading configuration is uniform. Nevertheless, the situation observed in practice is quite different: the loadings are rarely perfectly uniform and typical aircraft structural components are usually subjected to hundreds of load cases whose distributions are unlikely to be uniform.

There is one more issue of great concern: specification of the loading configuration may lead to optimal designs that are highly sensitive to variations in that configuration, i.e., if the loading is varied the design ceases to be optimal and may become flawed or unstable. Cherkaev and Cherkaeva [10] proposed a minimax technique to reduce or overcome the high sensitivity problem. They reformulate the optimization problem in such a way that the uncertainties in the loading are inherently part of the design variables. Their proposal ensures that the optimal designs obtained are less sensitive to variations in the loading configuration provided these variations obey certain integral bounds. The minimax technique applied to buckling maximization is more efficient if used in conjunction with the stability boundary theorem. They are not explained in detail in this work because this explanation can be found elsewhere [11] although they are essential to recognize the efficiency of the proposed strategy.

Apart from the loading uncertainty, the design of composite structures is complicated by the wide variety of matrix and fiber reinforcement materials available, the potential of stress concentrations, and thermal residual stresses from the manufacturing process. Particularly, thermal residual stresses may become so severe in thin heterogeneous composite plates that their effects cannot be overlooked if a truly reliable composite structure is to be designed. Moreover, it is possible to predict the thermal residual stress distribution with great accuracy [8] such that their effects can be not only avoided but also used to advantage in certain applications by properly tailoring the heterogeneous plate [9].

The loading configuration is not fixed in this paper but it is assumed to be described by piecewise linear functions defined along the plate edges. Hence, the entire class of loadings spanned by these basis functions is efficiently supported by the optimal designs obtained. In addition to the mechanical uncertain loads, the service temperature of the thin heterogeneous composite plate is also assumed to vary within a given range such that uncertain thermal loads must also be accounted for, i.e., the service temperature belongs to the vector of uncertain variables. Loading distributions other than piecewise linear may be approximated through consideration of more basis functions. Hence, the optimization problem is reformulated such that three sets of design variables are present: (i) the mechanical loading (basis functions), (ii) the service temperature, and (iii) piecewise constant thickness of the plate characterizing a heterogeneous composite design.

PLATE CONFIGURATION AND LOADING REPRESENTATION

A typical heterogeneous composite plate investigated is depicted in Fig. 1a where the piecewise constant thickness distribution can be observed in addition to the finite element mesh (dashed lines). In this particular sketch the heterogeneous plate has sixteen sub-regions with different total thicknesses. Figure 1a also shows a linear piecewise loading distribution along two opposite edges of the plate. Figure 1b illustrates a 3D view of the plate shown in Fig. 1a. It is assumed that the laminate has a total of eight layers with orientation $[0^o/90^o/0^o/90^o]_S$ such that the thicknesses of the four inner most plies are equal and constant. The 0° ply has its fibers aligned with the *x* axis in Figs. 1a-c. This kind of lay up can be regarded as a base plate with constant total thickness on top of which layers are added whose thicknesses may vary. The configuration can be visualized in Fig. 1b where the base plate is the dark region and the lighter regions represent the additional layers. Figure 1c shows sub-region *i* in detail with the ply thicknesses where the shaded plies have 0° orientation.

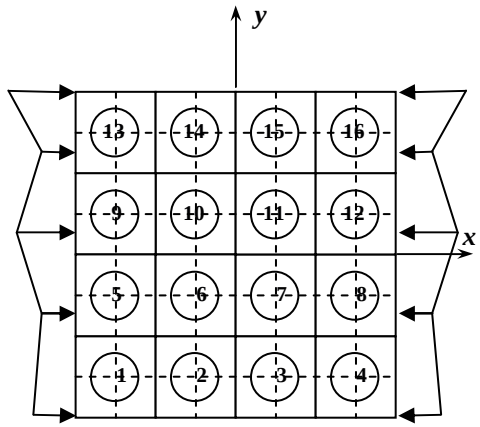

(a)

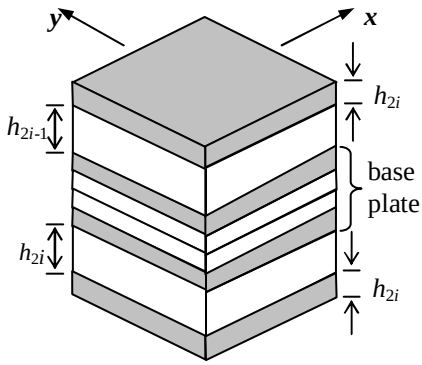

(b)

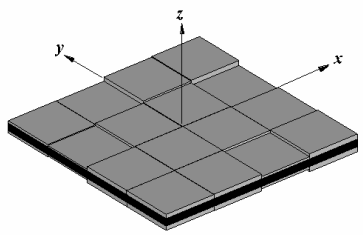

(c)

Figure 1 - Symmetric laminate composite plate with piecewise constant thickness

The piecewise linear loading shown in Fig. 1a is represented by a combination of basis functions defined at specific points. Figure 2a illustrates a general loading applied along one of the plate's edges. The piecewise linear basis functions are shown in Fig. 2b and are defined at five points. A proper combination of the magnitudes f_1, f_2, f_3, f_4 and f_5 (the heights of the triangles in Fig. 2b) represents the loading shown in Fig. 2a. Notice that the basis functions used to represent the loading distribution must not necessarily be defined at nodal locations as shown in Fig. 1a. However, in order to render the numerical procedures simpler, it is desirable to define the basis functions in relation to the nodal locations as shown in Fig. 2a.

The piecewise linear loadings are obtained by selection of f_1, f_2, f_3, f_4 and f_5. Any f_i is calculated as the product of a non-dimensional load parameter R_i times a scaling factor $\bar{f}_i$ as given in Eq. (1).

$$f_i = R_i \bar{f}_i \tag{1}$$

The load parameter R_i is within the interval [0,1] and provides a measure of the relative contribution of the *i*th basis function to the resulting net loading. The scaling factors are illustrated in Fig. 2c and must be selected such that the areas of the triangles in Fig. 2c are all the same and equal to some value $\bar{f}L$ where L is the length of the plate edge. Physically, this means all the resultant forces of each basis function have equal magnitude. Therefore, the resultant force produced by all the basis functions together has magnitude $F = \bar{f}L\sum R_i$ where m is the number of basis functions. If the load parameters correspond to the coefficients of a convex combination then the constraint expressed in Eq. (2) must be fulfilled and $F = \bar{f}L$. Additional discussion about the load parameters and the convex combination will be given in the following section.

$$\sum_{i=1}^{m} R_i = 1 \tag{2}$$

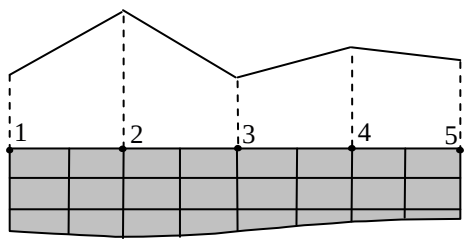

(a)

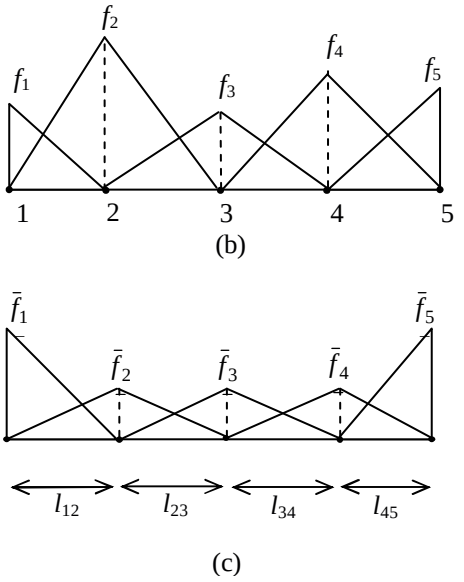

Figure 2: Uncertain piecewise linear loading

Calculation of the objective function λ (the buckling load) is divided into three steps: (i) solution of a linear thermal problem to obtain thermal residual stresses, (ii) solution of a linear prebuckling problem to obtain prebuckling mechanical stresses and (iii) solution of an eigenvalue problem to obtain the buckling load. Furthermore, the laminate is symmetric and assumed free of initial imperfections such that a bifurcation type of buckling is observed. The resulting thermal, prebuckling and buckling problems can be stated, respectively, in a compact form as

$$\mathbf{K}\mathbf{q}_t = \mathbf{f}_t \tag{3a}$$

$$\mathbf{K}\mathbf{q}_p = \mathbf{f}_p \tag{3b}$$

$$(\mathbf{K} + \mathbf{K}_t - \lambda \mathbf{K}_G)\mathbf{q} = \mathbf{0} \tag{3c}$$

where $\mathbf{K}$ is the stiffness matrix $\mathbf{q}_t$ are the thermal displacements, $\mathbf{q}_p$ are the prebuckling displacements, $\mathbf{f}_t$ is the global vector of thermal loads, $\mathbf{f}_p$ is the global vector of applied mechanical loads, $\mathbf{K}_G$ is the geometric stiffness matrix due to the nonlinear strains and prebuckling stresses, $\mathbf{K}_t$ is the geometric stiffness matrix due to the nonlinear strains and thermal residual stresses, and $\mathbf{q}$ is the buckling mode associated with eigenvalue λ.

OPTIMIZATION FOR UNCERTAIN PIECEWISE LINEAR LOADINGS

The resulting loading distribution is given by a convex combination of the basis functions illustrated in Figs. 2a-c. The force produced by each basis function F_i is expressed as in Eq. (4).

$$F_i = \lambda R_i \bar{f} L \tag{4}$$

where λ is the buckling load magnitude. Hence, the loading distribution is fully described by the load parameters R_i while the loading magnitude is given by λ and the value of $\bar{f}L$. In this work $\bar{f}L$ is made equal to unity without loss of generality. The shape of the mechanical loading is related to the load parameters whereas the thermal loading depends on the single parameter ΔT. Moreover, these loadings are assumed to be uncertain such that R_i and ΔT may be chosen arbitrarily although the load parameters must obey $0 \le R_i \le 1$ and Eq. (2), and ΔT is within a specified range $\Delta T_{\min} \le \Delta T \le \Delta T_{\max}$.

The danger associated with the loading uncertainty can now be appreciated. The traditional optimization procedure consists in selecting fixed R_i and ΔT and maximizing the buckling load magnitude λ against that particular loading configuration. However, if R_i and ΔT are varied, it cannot be guaranteed that λ will increase for the same design. Actually, if an unfortunate loading configuration is selected for a particularly sensitive design then the buckling load may become dangerously low or, even worse, thermal buckling may occur without even applying mechanical loads.

It is clear from the discussion above that the optimal design depends on the loading configuration, suggesting that the loading variability must be somehow incorporated in the optimization search. The optimization problem is reformulated as given by Eq. (5) in order to implement that suggestion.

$$\max_{\mathbf{h}} \min_{\mathbf{r},\Delta T} \lambda(\mathbf{h}, \mathbf{r}, \Delta T) \tag{5}$$

where $\mathbf{r} = (R_1, ..., R_m)$ is the vector of load parameters, $\mathbf{h}$ is the vector of thicknesses and has $2n$ components, n being the number of sub-regions of the plate as illustrated in Figs. 1a-c. Notice that the base plate has constant thickness

but the outer most 0° and 90° plies are assigned thicknesses h_{2i} and h_{2i-1} respectively as shown in Fig. 1c. One additional constraint exists involving **h** to enforce constant mass, i.e.,

$$\sum_{i=1}^{2n} h_i \le nh \tag{6}$$

where n is the number of plate sub-regions nh is the maximum thickness one ply can reach if all the others are zero

Solution of the minimax problem stated in Eq. (5) provides, simultaneously, the optimal design and the worst loading combination in terms of **r** and ΔT. This optimization problem is bilevel and its numerical solution is often laborious. However, the fact that λ is obtained through solution of the classic eigenvalue problem in Eq. (3c) allows for a tremendous simplification. Equation (5) can be rewritten as

$$\max_{\mathbf{h}} \phi(\mathbf{h}) \quad , \quad \phi(\mathbf{h}) = \min_{\mathbf{r},\Delta T} \lambda(\mathbf{h},\mathbf{r},\Delta T) \tag{7}$$

where evaluation of $\phi(\mathbf{h})$ is itself a minimization problem. Apparently, Eq. (7) does not introduce any simplification to the problem. However, if the extended stability boundary theorem is considered [11] then the computation of $\phi(\mathbf{h})$ is greatly simplified.

Figure 3 presents the sketch of the stability boundary surface for a fixed design **h**. This surface is obtained by variation of the load parameters R_i for a fixed ΔT and calculating λ. The shaded triangle observed in Fig. 3 is the reference plane that is the geometric representation of the convex combination constraint expressed in Eq. (2). The axes in Fig. 3 are the forces given in Eq. (4) when $\bar{f}L = 1$. As λ varies the reference plane moves away from the origin if $\lambda > 1$.

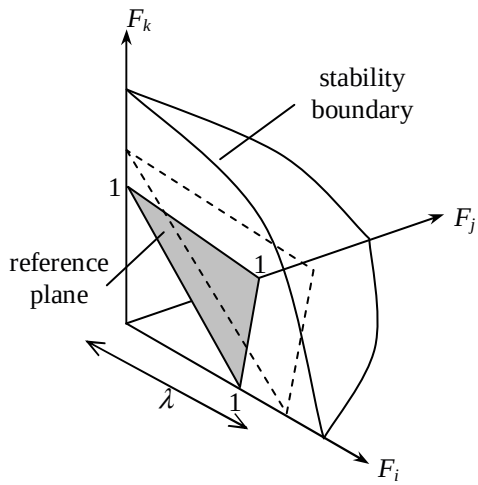

Figure 3: Stability boundary sketch

The stability boundary theorem guarantees that the stability surface is always concave provided $\mathbf{K}+\mathbf{K}_t$ is positive-definite and even when $\mathbf{K}_G$ is indefinite. If no thermal buckling has occurred than $\mathbf{K}+\mathbf{K}_t$ is certainly positive-definite. Since maximization of the buckling load is the objective the optimization search will not lead to designs that possess indefinite matrices $\mathbf{K}+\mathbf{K}_t$, thus making sure that the hypothesis of the stability boundary theorem is observed. Nevertheless, in order to be strictly certain, a Sturm check of $\mathbf{K}+\mathbf{K}_t$ is conducted for every design evaluated to ensure that positive-definiteness is present. This check adds little computational cost to the analysis because matrix $\mathbf{K}+\mathbf{K}_t$ must be decomposed anyway in order to obtain the eingevalues of the problem in Eq. (3c).

Computation of $\phi(\mathbf{h})$ is easily done for it is sufficient to evaluate λ at the points where the reference plane crosses the axes in Fig. 3. The concavity of the stability boundary surface automatically guarantees that any other loading configuration obtained through a convex combination of those points leads to higher λ. A similar argument can be employed to conclude that the whole interval of possible ΔT ($\Delta T_{\min} \le \Delta T \le \Delta T_{\max}$) must not be checked but only its ends: $\Delta T_{\min}$ and $\Delta T_{\max}$.

The optimization problem stated in Eq. (5) is in fact greatly simplified due to the concavity of the stability boundary surface. Numerical solution of the optimization problem is done in two steps: firstly 5,000 random designs are assessed in order to try and reduce the risk of convergence to local

optima, and secondly the best design randomly obtained is taken as the starting point for a Powell's search [14]. The choice of Powell's method over gradient-based nonlinear methods is motivated by simplicity. It requires neither the gradient of the objective function nor the gradients of the constraints. Therefore, Powell's method is adequate in this case because it is simple to implement and avoids potential complications due to derivatives of repeated eigenvalues. Moreover, the algorithm requires only continuity of constraints and objective-function, properties that the problem at hand presents. The optimization is assumed to have converged when the relative difference between the previous and present values of ϕ does not exceed 0.001.

NUMERICAL SIMULATIONS

A square plate simply supported along the four edges is considered for the numerical simulations. Notice that these boundary conditions apply to the mechanical problem stated in Eq. (3b) but for the thermal problem expressed in Eq. (3a) the plate is completely free to model the curing process. The plate edges are 36 cm long and the mechanical loadings are applied along the edges parallel to the y axis as shown in Fig. 1a. The base plate has 4 layers each one with constant thickness of 0.15 mm. The value of h expressed in Eq. (6) is 0.3 mm and, considering 16 sub-regions (n = 16), the maximum thickness one outer ply can reach is 4.8 mm. The material selected for simulations is given in Table 1. The processing temperature adopted is 120°C.

Table 1 – Material properties of the T300-5208 graphite/epoxy

property	value
Modulus of elasticity, E_{11}	154.0 GPa
Modulus of elasticity, E_{22}	11.13 GPa
In-plane Poisson's ratio, ν_{12}	0.304
In-plane shear modulus, G_{12}	6.98 GPa
Transverse shear modulus, G_{13}	6.98 GPa
Transverse shear modulus, G_{23}	3.36 GPa
Thermal expansion coef., α_1	-0.17×10^{-6} °C^{-1}
Thermal expansion coef., α_2	23.1×10^{-6} °C^{-1}

Comparison will be made considering the traditional optimal design obtained under fixed loading assumption the optimal design obtained by the minimax strategy introduced in Eq. (5) and re-written in Eq. (7). The fixed loading consists of the uniformly distributed load with a service temperature of 20°C such that $\Delta T = -100$°C. For the uncertain mechanical loading five basis functions are used as depicted in Fig. 2c and, assuming that the optimized plate will be mounted on an commercial jet, the service temperature ranges from –60°C and +80°C such that $-180°\text{C} \le \Delta T \le -40°\text{C}$.

The optimal thickness distributions obtained are given in Table 2. The traditional and the minimax optimal designs can be visualized in Figs. 4a and 4b, respectively. Symmetry of both optimal designs is observed about planes xz and yz. This result is expected because there is symmetry about planes xz and yz of the loadings and boundary conditions. In the case of the minimax strategy the basis functions are symmetrically defined about plane xz which translates into loading symmetry. Both optimal plates are reinforced along the plate central line parallel to the x axis where thicker sub-regions are present although different thickness distributions are obtained for the traditional and the minimax optimal designs. Also, the heterogeneous design is tailored such that the effects of the thermal residual stresses are beneficial but this is not as straightforward to recognize as the concentration of mass along the plate central line.

Table 2 – Optimal thickness distributions

	Traditional	Minimax
h_1, h_2 (mm)	0.00, 0.00	0.05, 0.01
h_3, h_4 (mm)	0.06, 0.00	0.09, 0.01
h_5, h_6 (mm)	0.06, 0.00	0.09, 0.01
h_7, h_8 (mm)	0.00 0.00	0.05, 0.01
h_9, h_{10} (mm)	0.08, 0.36	0.24, 0.28
h_{11}, h_{12} (mm)	0.00, 0.70	0.05, 0.47
h_{13}, h_{14} (mm)	0.00, 0.70	0.05, 0.47
h_{15}, h_{16} (mm)	0.08, 0.36	0.24, 0.28
h_{17}, h_{18} (mm)	0.08, 0.36	0.24, 0.28
h_{19}, h_{20} (mm)	0.00, 0.70	0.05, 0.47
h_{21}, h_{22} (mm)	0.00, 0.70	0.05, 0.47
h_{23}, h_{24} (mm)	0.08, 0.36	0.24, 0.28
h_{25}, h_{26} (mm)	0.00, 0.00	0.05, 0.01
h_{27}, h_{28} (mm)	0.06, 0.00	0.09, 0.01
h_{29}, h_{30} (mm)	0.06, 0.00	0.09, 0.01
h_{31}, h_{32} (mm)	0.00, 0.00	0.05, 0.01

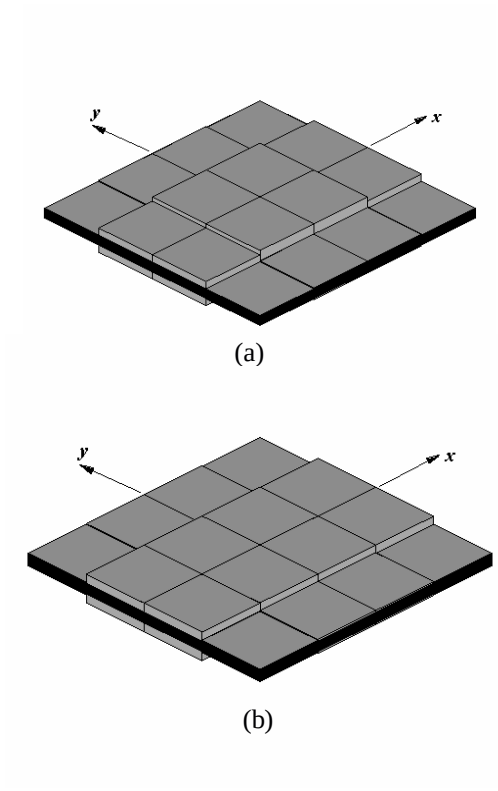

Figure 4: Optimal designs

Table 3 shows a comparative performance of the two optimal designs in terms of buckling loads (in N) obtained as both thermal and mechanical loadings are varied. The buckling loads associated with the load parameters R_4 and R_5 are not shown because they are equal to those associated with R_2 and R_1, respectively, in view of the symmetries mentioned above. It is obvious that the traditional design has superior performance when the loading is uniform and $\Delta T = -100^{o}$C because it is optimized for that particular situation. However, notice that in this case the minimax design yields λ = 1375.4 N, what is about 80% of the maximum λ = 1712.2 N. On the other hand, when R_1 = 1.0, $R_2 = R_3 = R_4 = R_5$ =0.0 and $\Delta T = -180^{o}$C the traditional design has poorer performance since it yields λ = 505.3 N what is only 55% of the minimax design's λ = 915.5 N.

Table 3 – Sensitivity of optimal designs

	ΔT (^{o}C)	R_1=1.0	R_2=1.0	R_3=1.0	uniform
Traditional	-180	505.3	876.3	1270.4	1720.6
	-100	524.9	886.4	1223.1	1712.2
	-40	536.2	888.3	1183.3	1691.7
Minimax	-180	915.5	943.1	962.1	1405.3
	-100	917.6	928.8	936.2	1375.4
	-40	914.3	914.3	914.3	1349.4

COMMENTS AND CONCLUSIONS

The minimax strategy proposed is applicable in the optimization of structures against buckling when multiple load cases are present or when the loadings are unpredictable. It is shown that for optimization purposes it is unnecessary to consider all the loads cases simultaneously but only a subset of them that contains the points where the reference plane intersects the axes associated with the basis functions as illustrated in Fig. 3. This property is particularly important whenever the multiplicity of load cases is so large that simultaneous consideration of them all leads to optimization problems so expensive computationally that they cannot be solved by the optimization algorithms available today in a reasonable time frame.

The minimax strategy can be regarded as a deterministic tool to study a probabilistic problem. It provides the engineer with optimal designs not based on probability distributions and averages but based on extreme properties of the systems under investigation. These extreme properties depend on the class of admissible loads chosen such it must be judiciously selected. The piecewise linear loads seem to be an adequate choice because it is at the same time simple and permits the representation of numerous load cases. If the class of loadings is to be expanded more basis functions may be added to the problem.

The load parameters R_i defined in Eq. (1) have equal probability of occurrence. However, it may be the case that a given loading configuration is more likely to appear. The idea to handle this situation is to split the load parameters into a certain component R_{0i} and an uncertain component ΔR_i such that $R_i = R_{0i} + \Delta R_i$. The certain component is invariant and represents the

loading configuration that is likely to occur. The uncertain components are perturbations of the most likely loading configuration. For instance, if the uniform loading is to be favored in the simulation conducted such that it has 50% probability of occurrence then $2R_{01} = R_{02} = R_{03} = R_{04} = 2R_{05} = 0.125$ and $\Sigma(\Delta R_i) = 0.5$. Minimization of ϕ in Eq. (7) is slightly different because now more points must be checked, not simply the points where the stability surface crosses the axes [11] but there is essentially no modification to the optimization strategy.

A finite element mesh of 8×8 elements was used to model the entire plate. Mesh refinement was done with 12×12 elements to make sure that the results obtained are reliable, i.e., that numerical approximations are acceptable. The element used was the bicubic Lagragian whose matrix is 80×80 such that relatively coarse meshes provide accurate results. Hence, the finer 12×12 mesh indicated small variations in terms of buckling loads (less than 3%) for all the basis functions.

ACKNOWLEDGEMENTS

This work was partially financed by the Brazilian agencies FAPESP (grant no. 2003/02863-4) and CNPq (grants 302112/2003-0 and 304642/2003-7).

REFERENCES

[1] Chao CC, Koh SL, Sun CT. Optimization of buckling and yield strengths of laminated composites. AIAA Journal 1975; 13(9): 1131-1132.

[2] Hirano Y. Optimum design of laminated plates under axial compression. AIAA Journal 1979; 17(9): 1017-1019.

[3] Haftka RT, Walsh JL. Stacking sequence optimization for buckling of laminated plates by integer programming. AIAA Journal 1992; 30(3): 814-819.

[4] Miki M, Sugiyama Y. Optimum design of laminated composite plates using lamination parameters. AIAA Journal 1993; 31(5): 921-922.

[5] de Andrade LH, de Almeida SFM, Hernandes JA. Optimization of buckling loads of thin reinforced orthotropic plates including the effect of thermal residual stresses. In: Proceedings of the Third World Congress of Structural and Multidisciplinary Optimization (WCSMO/3), Buffalo, NY, USA, 17-21 May 1999.

[6] Bruhn EF. Analysis and design of flight vehicle structures. Cincinnati: Tri-State Offset, 1973.

[7] Niu MCY. Airframe stress analysis and sizing. Hong-Kong: Hong Kong Conmilit Press, 2001.

[8] de Almeida SFM, Hansen JS. Enhanced buckling loads of composite plates with tailored thermal residual stresses. Journal of Applied Mechanics 1997; 64(4): 772-780.

[9] de Faria AR, Hansen JS. Optimal buckling loads of nonuniform composite plates with thermal residual stresses. Journal of Applied Mechanics 1999; 66(2): 388-395.

[10] Cherkaev E, Cherkaeva A. Optimal design for uncertain loading conditions. In: Berdichevsky V, Jikov V, Papanicolaou G, editors. Homogenization. Singapore: World Scientific, 1999, p. 193-213.

[11] de Faria AR, Hansen JS. On buckling optimization under uncertain loading combinations. Structural and Multidisciplinary Optimization Journal 2001; 21(4): 272-282.

[12] Daniel IM, Ishai O. Engineering Mechanics of Composite Materials. London: Oxford University Press, 1994.

[13] Koiter WT. On the stability of elastic equilibrium. PhD thesis, 1945. English translation: Air Force Flight Dynamics Technical Laboratory, Report AFFDL-TR-70-25, Feb. 1970.

[14] Vanderplaats GN. Optimization Techniques for Nonlinear Engineering Design with Applications. New York: McGraw-Hill, 1984.